Computer Modeling of Packing Arrangements and Transitions in Saturated-*cis*-Unsaturated Mixed Triglycerides

J.W. Hagemann* and **J.A. Rothfus**

Biopolymer Research, National Center for Agricultural Utilization Research, U.S. Department of Agriculture, Agricultural Research Service, Peoria, Illinois 61604

Conformational analysis of modeled *cis*-unsaturated chains in triunsaturated and symmetrical monounsaturated triglycerides has identified pseudo-linear chain orientations that allow lower molecular mechanical energies than are possible with conventional *cis*-chains. Energy plots recorded during bond rotations near the double bond show that energy barriers between linear and normal *cis*-configurations are often less than 5 Kcal/mol. Pseudo-linear orientations, which allow compatible side-by-side packing of saturated and unsaturated chains in double-chainlength mixed triglycerides, also provide a route for efficient transformation between double-chainlength and triple-chainlength configurations in solid polymorphic triglycerides.

KEY WORDS: Computer modeling, double-chainlength, molecular mechanics energy, phase transitions, polymorphism, tri-*cis*-11-eicosenoin, triglycerides, triple-chainlength.

One of many unanswered questions regarding triglyceride polymorphism concerns the phase transitions of saturated-unsaturated mixed triglycerides (*e.g.*, oleoyl distearin, SOS, and oleoyl dipalmitin, POP), (1,2). Recent studies by Gibon, Durant and Deroanne (3) and Sato *et al.* (4) on the thermal transitions of mixed triglycerides reveal dramatic reversible changes in X-ray long spacings that would be consistent with a substantial increase in the distance between molecular end group planes and a shift in molecular arrangement from double- to triple-chainlength configurations of the type illustrated in Figure 1(b). Such molecular transformation allows unsaturated chains to pack with other unsaturated chains in the triple-chainlength configuration, but in double-chainlength arrangements saturated and unsaturated chains must pack side-by-side, presumably in chain orientations quite different from that normally associated with *cis*-unsaturated structure. Insight into how such molecular arrangements might arise and contribute to unusual dimensional shifts of crystalline lipids is allowed by computer-aided analysis of *cis*-chain orientations in unsaturated triglycerides.

EXPERIMENTAL PROCEDURES

Chain and atom labeling. A schematic of the triglyceride structure used in these modeling studies is shown in Figure 1(a). Chains are numbered according to Lutton (5). Individual atoms in each chain are numbered from the terminal methyl carbon (*i.e.*, chain #1 equals 1 through 20; chain #2, 21 through 40; and chain #3, 41 through 60). Double bond locations are identified according to standard convention for fatty acids, in which the carbonyl carbon is number one. Thus, for example, Δ11 unsaturation in chain #3 of Figure 1(a) occurs between carbons 49 and 50 of the triglyceride model.

Unsaturated bond orientations. Tri-*cis*-11-eicosenoin was modeled in a symmetrical tuning fork arrangement, Figure 1(a), from triarachidin (6) by removing hydrogen atoms to create *cis*-Δ11 unsaturation. The unsaturated carbon-carbon bond distance was adjusted to 1.34 Å. Initially, each unsaturated chain was oriented with an average 137° bend at the *cis* bond. To search for low-energy conformational forms, portions of the triglyceride were treated as separate entities. Chain #2 [Fig. 1(a)] was altered independently, but changes made in chain #1 were made simultaneously in chain #3 to achieve synchronous movement and to avoid chain contact and overlap.

Carbon-carbon bonds were rotated in 5- or 10-degree increments except near energy minima, where rotations were reduced to 1 or 2 degrees. Bond rotations were confined to the adjacent single bonds on either side of the double bond to keep the bulk of each chain segment in an all-*trans* configuration. This constraint, which essentially expresses any scattered *gauche* orientation effects as four equivalent single bond rotations, is not inconsistent with predominant *trans* methylene orientation observed by X-ray. It also was favored due to practical limits on computation times. Bonds nearest the glycerol region were rotated first; *i.e.*, C_{11}-C_{12} and C_{51}-C_{52} for chains #1 and #3, and C_{31}-C_{32} for chain #2. The low-energy form, having a normal *cis* orientation identified by the first rotations, *i.e.*, C_{11}-C_{12} and C_{51}-C_{52} bonds, was used as a starting point for the next set of bond rotations, C_{10}-C_{11} and C_{50}-C_{51}.

Mixed saturated-unsaturated triglycerides. A 2-oleo-1,3-distearin molecule (SOS) was prepared from a triarachidin model. Two methylene units were removed from each chain, and the double bond was placed in the Δ9 position of chain #2. For best-fit and transformation studies, the low-energy configuration found for chain #2 in tri-*cis*-11-eicosenoin was assigned to the SOS molecule.

Arrangements and transitions. Minimum energy positions for two molecules in both the double- and triple-chainlength arrangements were determined by placing the molecules in close proximity in an arbitrary starting position. One molecule remained stationary while the other was allowed movement along the X-, Y- and Z-axes, and rotation about the long verticle Y-axis through the central glycerol carbon until a minimum energy position was found. Between values for initial and final axes positions, whole molecule rotations and bond rotations were divided into 100 steps. At each step, mathematically adjusted parameters were incremented a portion of their total value, and the molecular mechanics energy (MME) was calculated to produce an energy curve for the transition.

Modeling system. The Chem-X molecular modeling system, developed and distributed by Chemical Design Ltd. (Oxford, England), was used for bond rotations, axes shifts, calculation of MME's (7) and display studies of orientations and transitions. A Digital MicroVAX 2000 computer (Digital Equipment Corp., Marlborough, MA) and a Tektronix 4225 high-resolution terminal (Tektronix Inc., Beaverton, OR) were used to run the Chem-X software.

*To whom correspondence should be addressed at NCAUR, 1815 N. University St., Peoria, IL 61604.

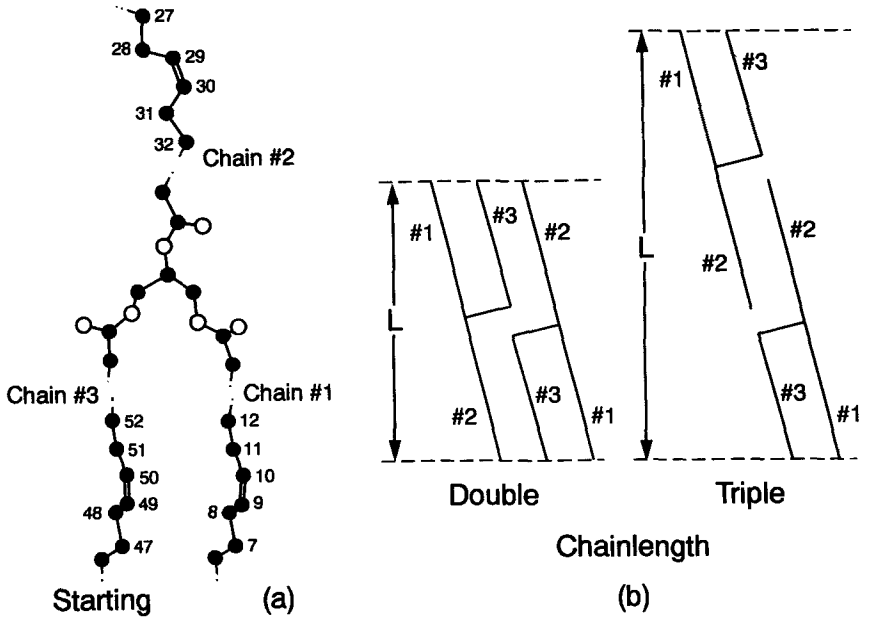

FIG. 1. Triglyceride structures. (a) Chain and atom labeling used for *cis* chain orientation studies. Chains are numbered according to the convention of Lutton (5). Carbon atoms are filled circles, oxygen atoms are open circles, and hydrogen atoms are not shown. (b) Schematic drawings of double- and triple-chainlength triglyceride structures. L equals long spacing distance.

RESULTS

Crystalline monoacid triglycerides, both saturated and unsaturated, generally occur in double-chainlength (DCL) structures [refs. 8–10; Figure 1(b)], which have long spacings, L, approximately equivalent to the length of two extended fatty acid chains. This methyl-to-methyl distance is reduced when chains are tilted with respect to the methyl group plane. As the name implies, triple-chainlength (TLC) structures have a long spacing that approximates the length of three fatty acid chains minus a reduction for chain tilt. In TCL structures of POP and SOS, the oleic acid moieties (chain #2) pack together, thereby segregating saturated and unsaturated chains in stable, high-melting polymorphs. If a normal *cis* orientation were maintained in DCL structures, side-by-side packing of saturated and unsaturated chains should produce many voids in the crystal lattice and result in unstable liquid-like substances. Yet DCL forms of saturated-unsaturated mixed triglycerides are relatively stable and display definite melting points and X-ray spacings (4).

Low-energy forms of chains #1 and #3. A flow chart of transformations employed during the search for optimal energy forms of chains #1 and #3 is shown in Figure 2, which identifies bonds rotated, the extent of rotation at an energy minimum, the observed MME in Kcal and, in schematic, the general shape of the molecule.

Rotating bonds C_{11}-C_{12} and C_{51}-C_{52} in chains #1 and #3 at −72° disclosed a nearly linear configuration that had a MME slightly lower than the MME's for either of the other forms, normal *cis* or pseudo-linear. An energy plot for rotation about these bonds is given in Figure 3, which also shows the distance between methyl groups C_1 and C_{41} in chains #1 and #3, respectively, during bond rotation. MME's for the normal *cis* orientation at 19° and the pseudo-linear structure at −72° differ by 3.3 Kcal but, as Figures 2 and 3 reveal, the two forms are separated by an energy barrier of approximately 8 Kcal. A larger 22-Kcal barrier separates the −72° structure from an unusual, though apparently stable, orientation at −222°. The C_1:C_{41} distance, indicative of chain spacing, shows that the closest approach of end groups on chains #1 and #3 coincides with conformational stability, which occurs at −72° when the end groups are separated by 4.45 Å. This spacing approximates the 4.15 Å short spacing for α-forms of saturated monoacid triglycerides (11), the 4.21 Å spacing for α-forms of SOS and POP (1,4), and the 4.36 Å spacing for α-forms of triolein (12).

Rotation about the C_{10}-C_{11} and C_{50}-C_{51} bonds of chains #1 and #3 (Fig. 4) also proved interesting. It produced two distinctly different orientations, 45° and −18°, separated by a barrier of less than 1 Kcal and slightly lower in energy than the 19° starting structure (Fig. 4). Together these interconvertable orientations represent a conformational switch point from which molecules might proceed *via* different paths to ultimately different configurations. In the present case, additional C_7-C_8:C_{47}-C_{48} rotations led to minimized structures with slightly lower MME's. A final normal *cis* structure at 21° was about 1.5 Kcal lower in energy than an analogous counterpart at 9°. Both were separated from quite different configurations by 5 Kcal barriers.

Low-energy forms of chain #2. The search for low-energy

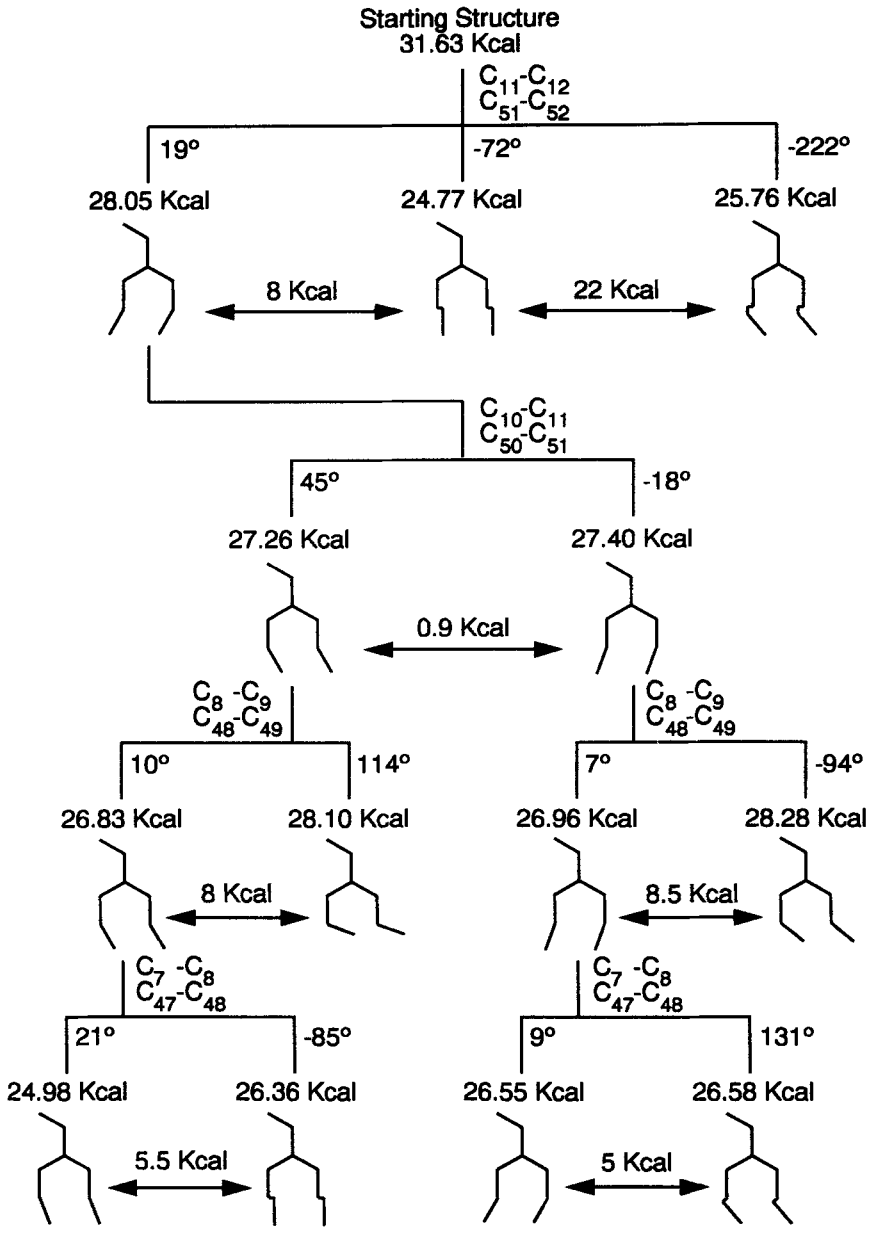

FIG. 2. Flow chart of search for low-energy forms of chains #1 and #3 in tri-*cis*-Δ11-eicosenoin in terms of bonds rotated, degree of rotation at energy minimum, molecular mechanics energy (Kcal) and schematic triglyceride shape. Double arrows indicate energy barriers between orientations.

normal *cis* and pseudo-linear forms of chain #2 began with the same initial structure [Fig. 1(a)] used in the analysis of chains #1 and #3. Figure 5 details the bond rotations applied to chain #2. Rotation about the C_{31}-C_{32} bond produced a normal *cis* orientation at −21° and a pseudo-linear form at 80° separated by an energy barrier of 8 Kcal, which is identical to the barrier between normal *cis* and pseudo-linear forms of chains #1 and #3 (Fig. 2).

C_{10}-C_{11}:C_{50}-C_{51} rotations in chains #1 and #3 produced two normal *cis* forms. However, rotation of the equivalent bond, C_{30}-C_{31} in chain #2, formed one normal *cis* configuration and two orientations with acute bends in the chain. On the proximal side of the double bond in chain #2, rotations of the C_{28}-C_{29} bond did not produce a normal *cis* orientation, and were a useless source of starting structures for C_{27}-C_{28} rotations. Forms generated from the C_{30}-C_{31} −16° configuration by rotation of the C_{27}-C_{28} bond to 88° and −124° also appeared linear. But when viewed from another angle (Fig. 5), these structures exhibited a more normal *cis* bend and, therefore, were not true pseudo-linear forms.

Minimal energy forms. Final low-energy configurations

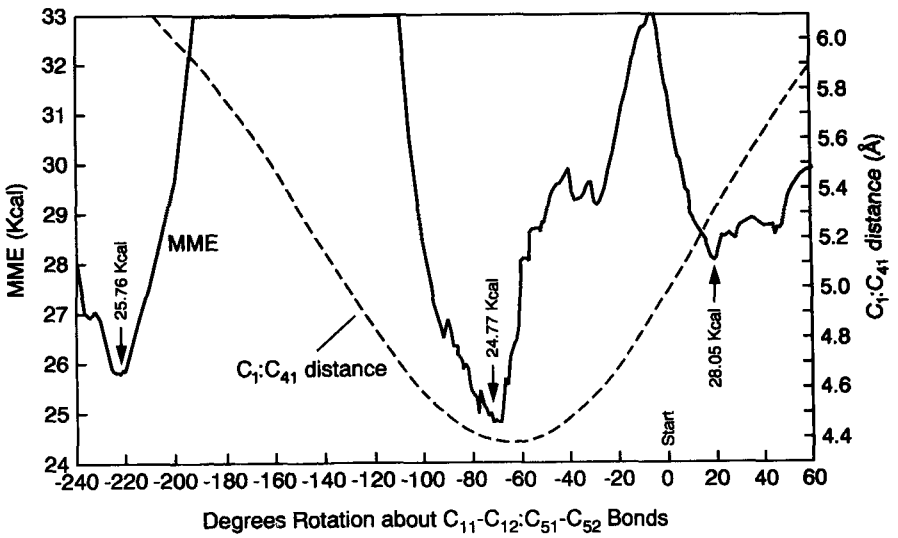

FIG. 3. Molecular mechanics energy of rotation (solid line) about C_{11}-C_{12} and C_{51}-C_{52} bonds, and methyl group distance (dashed line) between C_1 and C_{41} on chains #1 and #3, respectively. Arrows indicate energy minima.

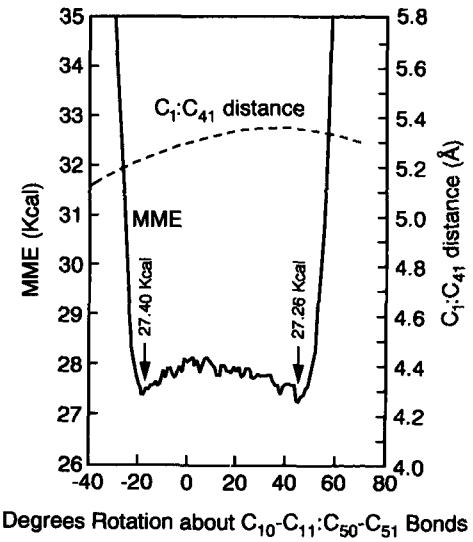

FIG. 4. Molecular mechanics energy of rotation (solid line) about C_{10}-C_{11} and C_{50}-C_{51} bonds, and methyl group distance (dashed line) between C_1 and C_{41} on chains #1 and #3, respectively. Arrows indicate energy minima.

for pseudo-linear and normal *cis* structures were obtained by combining bond rotations identified in the analyses of chain conformations (Figs. 2 and 5). Skeletal drawings of three of these structures are shown in Figures 6–8. The MME, 23.43 Kcal, of the lowest-energy linear form (Fig. 6) is lower than that for any of the other configurations. This minimal structure was derived by a −72° rotation in chains #1 and #3 (Fig. 2) and an 80° rotation in chain #2 (Fig. 5). Carbon-carbon zigzag planes approximately perpendicular to each other on opposite sides of the double bond are an interesting feature clearly shown by the two views in Figure 6. A similar (MME, 23.61 Kcal), though less linear, form (not shown) can be made by combining a −72° rotation in chains #1 and #3 (Fig. 2) with rotations of −21°, −16° and −124° in chain #2 (Fig. 5).

Figures 7 and 8 each show two views of low-energy forms (MME, 23.55 and 23.62, respectively) that have nearly normal *cis* bends in the acyl chains. Chain #2 of the structure in Figure 7 contains one unusual bond orientation, C_{28}-C_{29}, but MME calculations indicate that this is a low-energy conformation. Chains #1 and #3 of both structures were derived by the 19°, 45°, 10° and 21° rotations of Figure 2. Chain #2 of Figure 7 resulted from −21°, −16° and 88° rotations, whereas the structure in Figure 8 was made by −21°, −16° and −19° rotations. The two structures differ most in the chain #2 configuration. Carbon-carbon zigzag planes on opposite sides of the *cis* bond are approximately perpendicular in Figure 7 but are nearly parallel in Figure 8.

DCL to TCL conversion. Conversion of the SOS molecule from DCL to the TCL arrangement required that chain #2 of each molecule start in the pseudo-linear orientation and end in the normal *cis* configuration. A total of nine parameters, which included bond and whole-molecule rotations and axes shifts, were changed at each step in the conversion. Initial experiments with linear change in each parameter, *i.e.*, with each step equal to 1/100th of the total change of each parameter, produced unrealistically high MME values due to close approaches and, sometimes, overlap in portions of the molecule.

Comparing initial and final structures in Figure 9, it is evident that one molecule must move upward (Y = 24.5 Å) and to the left (X = −6.4 Å), while both molecules are rotated on axes (Z-axis) vertical to the plane of the Figure, one molecule clockwise and the other counterclockwise about glycerol centers. Review of conditions at intermediate steps in the initial linear-increment experiments suggested that delays in the X-axis shifts and Z-axis rotations (through an increasing function), combined with relatively large initial Y-axis shifts (a decreasing function), might eliminate atom-atom overlap and reduce total

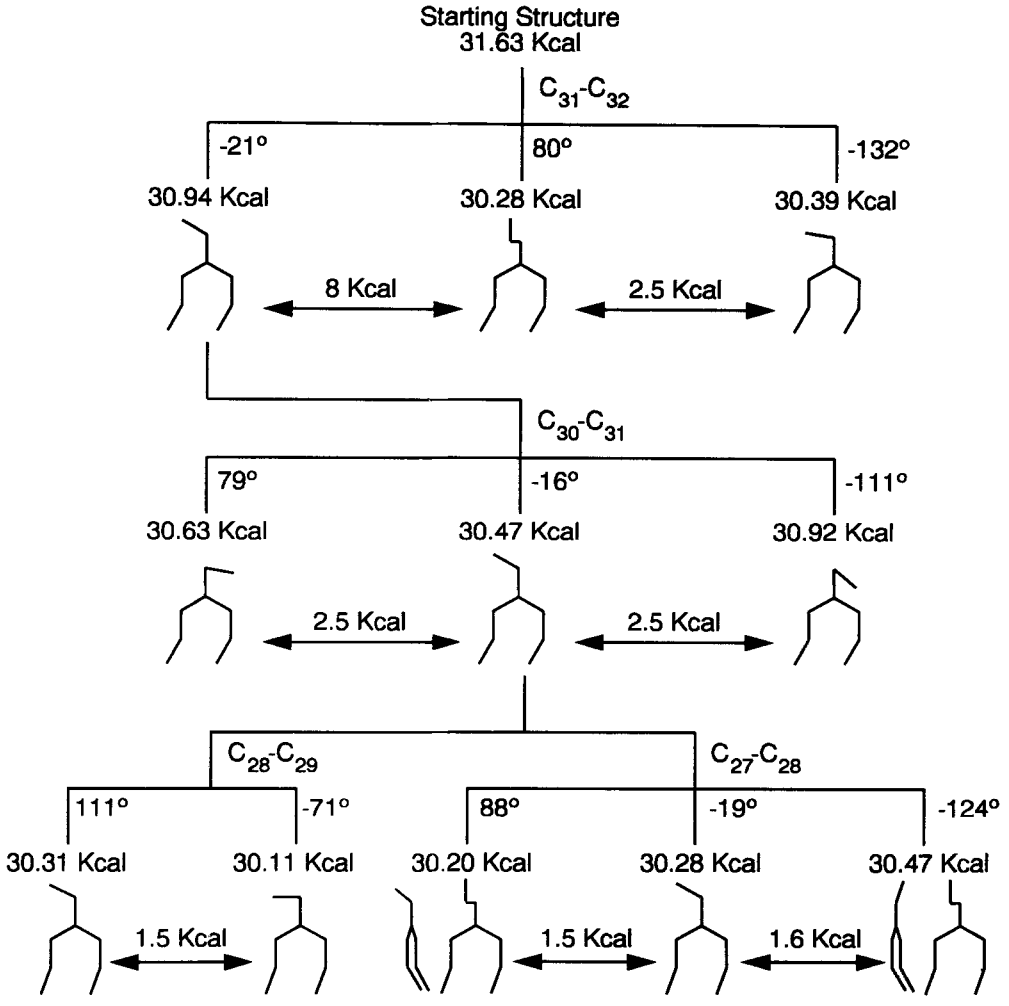

FIG. 5. Flow chart of search for low-energy forms of chain #2 in tri-*cis*-Δ11-eicosenoin in terms of bonds rotated, degree of rotation at energy minimum, molecular mechanics energy (Kcal), and schematic triglyceride shape. Double arrows indicate energy barriers between orientations.

MME. Parameter values at each of the 100 steps were calculated as follows:

$$\text{X-shift/Z-rotation} = [(F-S)/(\text{Total steps})^2] \times (\text{Step No.})^2$$

$$\text{Y-shift} = [(F-S)/(\text{Total steps})^2] \times [(\text{Total steps} + 1) - \text{Step No.}]^2$$

where F and S are final and starting value.

Effects of these adjustments are reflected in computer-generated images of molecular positions at every 20th step of the transition (Fig. 9), and in the energy curve for the DCL to TCL conversion (Fig. 10). Contact between oleic acid and the adjacent molecule is eliminated and, at the same time, the overall spacing between molecules remains relatively constant. The energy profile for the first half of the conversion (Fig. 10) shows a series of high-energy transitions, which may or may not arise from interactions representative of activation processes. Overall, the energy barrier (approximately 34 Kcal) presented by these high-energy intermediate steps is not inconsistent with apparent phase excitation energies for monoacid triglycerides (13).

DISCUSSION

Previous modeling studies (6) have shown that several tuning-fork arrangements meet a requirement for α-forms of saturated triglycerides; namely, symmetry in the glycerol region (14). Little else, however, is known in detail of α-form structure, even though many studies have focused on the polymorphism of saturated mono-acid triglycerides (15). Even less is known about mixed saturated-unsaturated triglycerides. Thus, any of the proposed theoretical α-forms (6) is suitable for examining the feasibility of chain packing alternatives and possible conversion pathways for saturated-unsaturated triglycerides. Our findings affirm the conviction that subtle molecular differ-

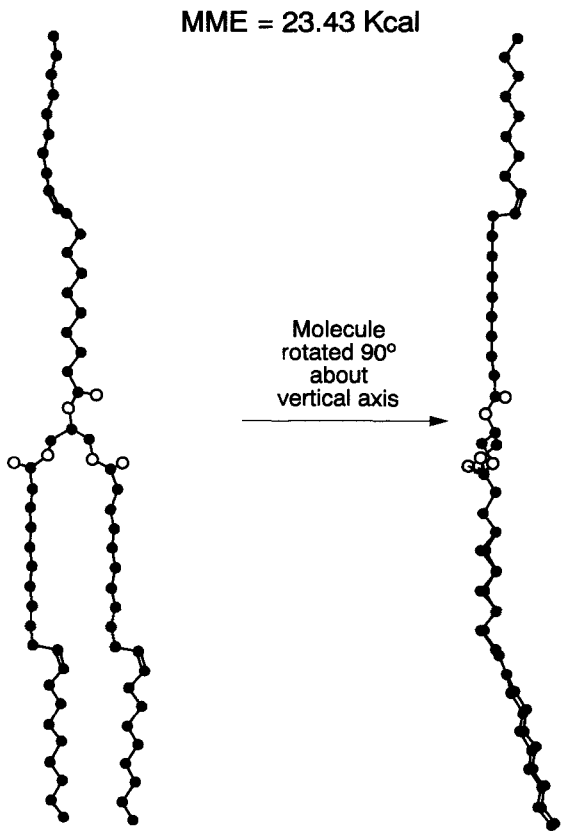

FIG. 6. Low-energy form of a pseudo-liner *cis*-unsaturated triglyceride. Carbon atoms are filled circles, oxygen atoms are open circles, and hydrogen atoms are not indicated.

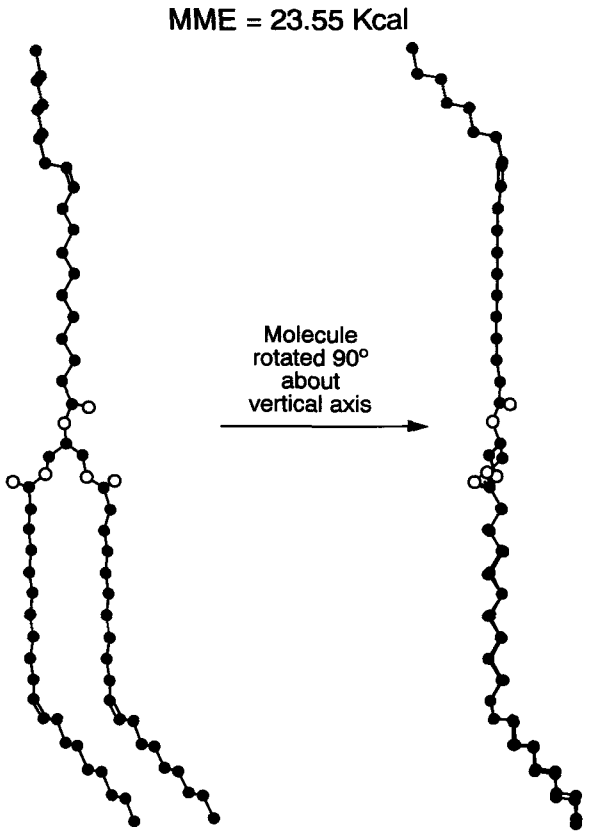

FIG. 7. Low-energy Form I of a *cis*-unsaturated triglyceride. Carbon atoms are filled circles, oxygen atoms are open circles, and hydrogen atoms are not indicated.

ences regulate lipid behavior. Logically, knowledge of how minute kinetic and energetic differences segregate lipid populations is the key to selective exploitation of lipid properties.

Most of the minimal configurations identified for chains #1 and #3 (Fig. 2) and chain #2 (Fig. 5) differed little from each other in terms of calculated mechanical energy. MME's for configurations in Figure 2 (chains #1 and #3) averaged 4.9 Kcal less than that for the starting configuration; extremes were separated by 3.5 Kcal. Similarly, MME's for chain #2 were reduced from the starting value by only 1.2 Kcal, on average, and were spread over a range of 0.8 Kcal. MME's calculated for minimized whole-molecule configurations (Fig. 6–8) were consistent with the energy reductions achieved by selected bond rotations in the separate chains. It is possible that several of these minimal molecular forms, though somewhat unusual in shape, may coexist in lipid populations during polymorphic transitions. It remains to be seen how many will be observed by improved detection methods.

The minimal structures identified in this study present evidence for two especially interesting features: i) Pseudo-linear alkene chains with *trans* bond orientation adjacent to the double bond; and ii) nonparallel zigzag planes on opposite sides of *cis* bonds. Pseudo-linear alkene chains, as illustrated in Figure 6, are not theoretical curiosities. A similar conformation was reported by Sawzik and Craven after X-ray analysis of cholesteryl nervonate (16) and cholesteryl palmitoleate (17). de Jong (18) also recognized the feasibility of overall straight configurations for unsaturated triglycerides with a *trans-skew-cis-skew-gauche* torsion angle sequence through the double bond (*gauche* = ± 60°; *skew* = ± 120°; *trans* = 180°; *cis* = 0°). DeJong pointed out that single bonds adjacent to a *cis* double bond cannot be *cis*. His analysis of available X-ray data on *cis* unsaturated compounds further suggested that the *skew* conformation would be favored for such single bonds.

Bond torsion angle data in Table 1 are consistent with such observations, but they suggest that angles adjacent to the double bond will be nearer *trans* and *skew*, which would affect the ability of the molecule to pack orderly among neighboring molecules. Significantly, one of two independent molecules in the unit cell of cholesteryl palmitoleate (17) exhibits a single bond torsion angle of −165° adjacent to the double bond, which is essentially identical to the preferred conformation (± 167° ave.) at double bonds in the pseudo-linear form identified by this study. In the identified favored configurations (Table 1), chains #1 and #3 are nearly identical to each other, which emphasizes the advantage of similar structure in adjacent chains. Chain #2 is approximately the same except for the direction of rotation and the C_{26}-C_{27}-C_{28}-C_{29} angle of Form I.

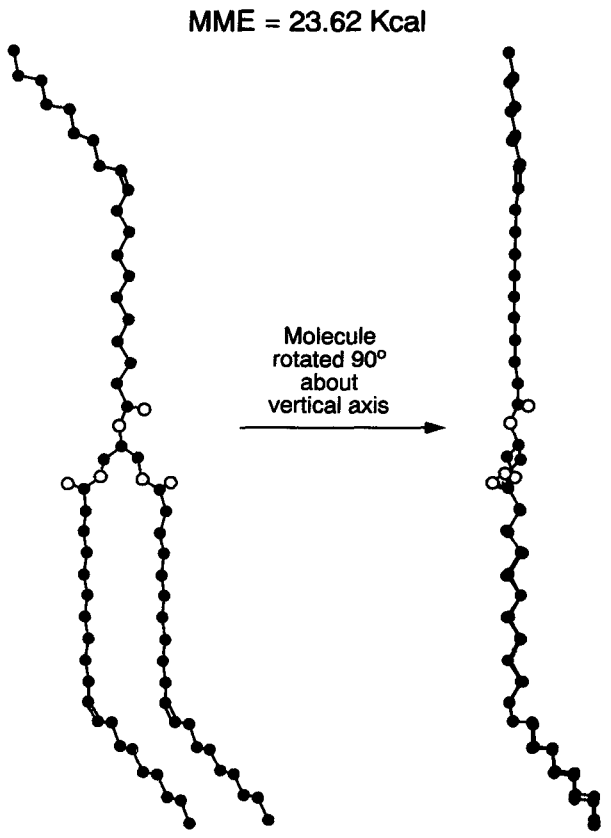

FIG. 8. Low-energy Form II of a *cis*-unsaturated triglyceride. Carbon atoms are filled circles, oxygen atoms are open circles, and hydrogen atoms are not indicated.

Elements of structure in Figures 6–8 are similar to those found in single crystal studies of oleic (19) and erucic (20) acids, which show parallel zigzag planes on opposite sides of the *cis* double bond. Chains #1 and #3 in Figure 7 exhibit this structure, as do the three chains of the second low-energy normal *cis* structure in Figure 8. In Figures 7 and 8, however, portions of the chains between the double bonds and methyl groups at opposite ends of the molecule point in directions approximately 180° from each other. This is similar to the pattern found for double chain layers of oleic and erucic acids hydrogen bonded through their carboxyl groups.

Nonparallel zigag planes on opposite sides of *cis* bonds are prominent in the pseudo-linear structure (Fig. 6) and chain #2 of Form I (Fig. 7). This segmented chain configuration was proposed originally to rationalize the observation of multiple β'-forms for some triglycerides and the absence of β'-forms for others during differential scanning calorimetry of monoacid *cis* triglycerides (21). It is comforting to find, two decades later, that such unusual structure is indeed preferred in low-energy forms. X-ray data indicate that zigzag planes alternate in β'-forms (9). Perhaps chain configurations of the type shown in Figure 7 do contribute to the polymorphic behavior displayed by all-*cis* and mixed triglycerides.

Unfortunately, little information is available by which to evaluate models composed of 20-carbon *cis*-unsaturated chains (Figs. 6–8). A shorter molecule, triolein, can be made by removing two methylene units, approximately 2.5 Å per repeating unit (22), from the vertical zigzag portion between glycerol and the double bond of each chain. A shortened molecule's vertical axis length should approximate known X-ray long spacing dimensions for C18 triglycerides. Long spacing values reported for triolein α-forms vary from 44.8 to 47 Å; β'-forms, 44.8 to 45.8 Å; and β-forms, 43 to 45 Å (12,23,24). While there is no evidence that α-triolein has pseudo-linear chains like those in Figure 6, the length of the triolein model, 44.2 Å, approximates the lowest reported long spacing value. Models with nearly normal *cis* bends, Figures 7 and 8, have lengths (approximately 40.2 Å) 3–5 Å shorter than those reported for β-forms, but this small difference can easily be corrected by a slight change in the angle of chain bend at the *cis* bond. Increasing the angle adjacent to each double bond by 2° will increase the long spacing by nearly 0.7 Å and the chain bend approximately 2.7°.

Better agreement with known dimensions was found by comparing published X-ray long spacings (4) to lengths for modeled DCL and TCL structures of SOS. In Figure 9, the starting (α-2) structures assigned pseudo-linear configurations (Fig. 6) have an overall length of 48.1 Å, which compares well with a recently reported X-ray value of 48.3Å. The observed length is slightly longer than the single molecule length because one molecule is shifted slightly with respect to the other in the long axis direction to improve interaction energetics. The final TCL structures in Figure 9 have an oberved overall length of 67.6 Å as compared with X-ray values of 65.0 Å for β and 70.0 Å for β' (4). The model essentially represents an average of β and β' dimensions. Again, the precise molecular length depends on the *cis*-bend angle. This close correlation between modeled and observed long spacings lends credence overall to the schematic mechanism in Figure 9, but much remains to be learned about how intermolecular forces focus and redistribute to compel the drastic DCL to TCL change in configuration. Processes leading to α-form activation likely determine when and at what rate the transition occurs. Accordingly, further modeling will consider interactions that might promote or inhibit the bond rotations summarized in Figure 9. Final structural proof will most likely depend on single crystal X-ray, but ^{13}C-nuclear magnetic resonance, which is sensitive to *gauche* configurations, also could prove benefical.

Obviously, polymorphic transitions occur in temporal environments composed of different rate processes. Therefore, algorithms that incorporate kinetic parameters are appropriate. Adjusting molecular shifts and rotations relative to one another maintained molecular proximity and reduced the transition energy barrier substantially to about 34 Kcal (Fig. 10). In unadjusted transitions, individual steps produced six-digit energy values due to atom-atom contact. Throughout the first half of the parameter-adjusted transition (Fig. 10), energy peaks occurred at steps 13, 19, 25, 32 and 39 when protons near the end of *cis*-chain #2 passed close to protons on the adjacent saturated chain (Fig. 10, steps 20 and 40). By Step 60, *cis*-chain methyl protons on the upper SOS molecule clear the saturated chain of the lower molecule and little remains to interfere with concerted collapse into a more stable configuration. From the general shape of the curve

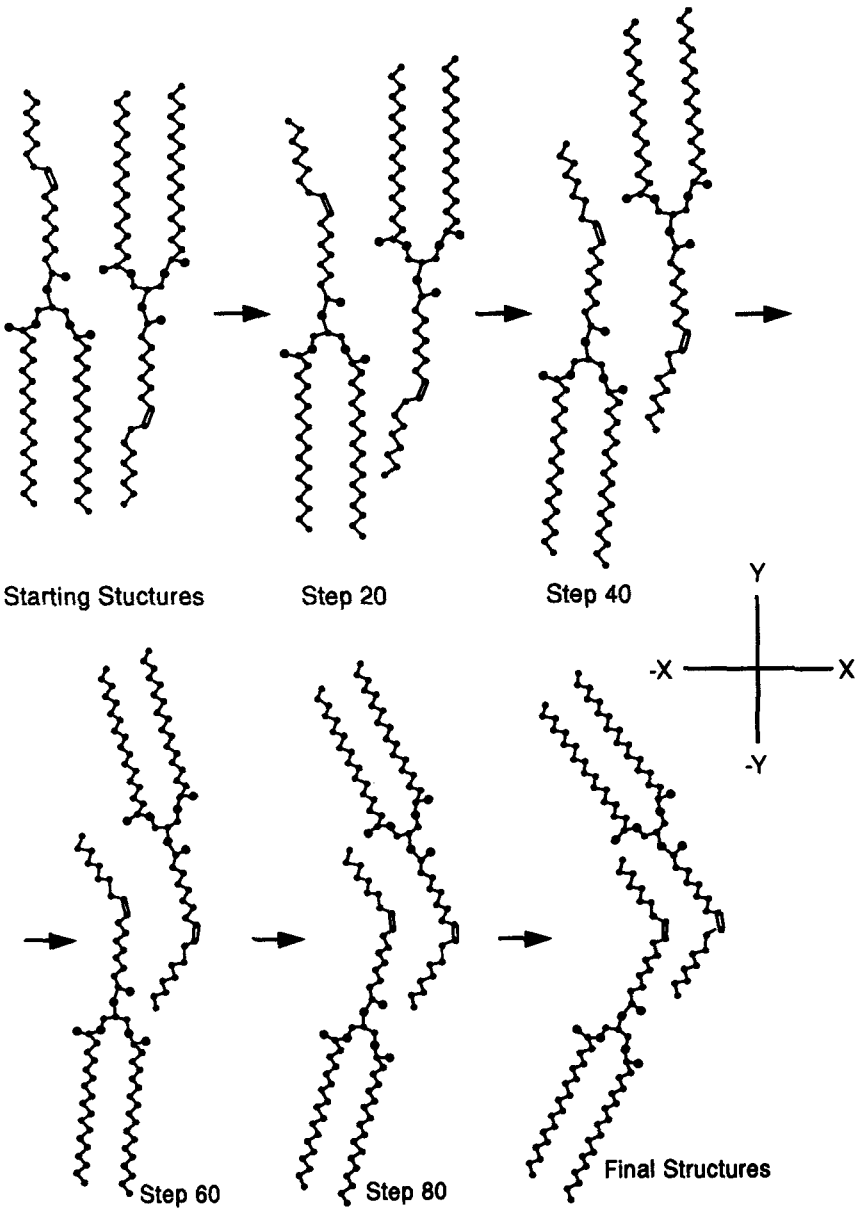

FIG. 9. Speculative scheme for DCL to TCL conversion of SOS. Molecular orientations are shown at every 20th step. Carbon atoms are filled circles, oxygen atoms are open circles, hydrogen atoms are not indicated.

in Figure 10, it appears that added experimentation with kinetic adjustments might further reduce the energy spikes, and that the activation energy for a DCL to TCL conversion of SOS might be near 15 Kcal.

These computational experiments intentionally explored options available to unsaturated chains in triglyceride configurations that represent but a few of many that might be consistent with accepted knowledge of crystalline lipids. Systematic extensions of such analyses that identify local features of defined molecular contexts will, in turn, provide larger contexts in which to conduct the more difficult search for conditions that regulate transformations into and out of global minima in lipid populations. The current experiments, for example, do not consider changes in the glycerol region, which might also contribute to DCL to TCL conversions. Some such additions may be necessary to account for X-ray data that evidence a rather more complex DCL to TCL to DCL conversion in the SOS homologue POP (4). Within the defined context, however, the work identifies low-energy configurations in which unsaturated chains pack efficiently with saturated chains, and it provides an appealing mechanism by which such triglyceride populations could undergo polymorphic transitions in unison through relatively simple bond rotations with a minimum of molecular separation.

TABLE 1

Torsion Angles Around *cis*-Bonds of Theoretical Unsaturated Triglycerides

Torsion angle	Pseudo-linear[a]	Normal	
		Form I[b]	Form II[c]
Chain #1			
C_6-C_7-C_8-C_9	−160	179	179
C_7-C_8-C_9=C_{10}	−171	179	179
C_8-C_9=C_{10}-C_{11}	0	0	0
C_9=C_{10}-C_{11}-C_{12}	−164	151	151
C_{10}-C_{11}-C_{12}-C_{13}	−80	−171	−171
Chain #2			
C_{26}-C_{27}-C_{28}-C_{29}	157	69	176
C_{27}-C_{28}-C_{29}=C_{30}	−159	−159	−159
C_{28}-C_{29}=C_{30}-C_{31}	0	0	0
C_{29}=C_{30}-C_{31}-C_{32}	168	−176	−176
C_{30}-C_{31}-C_{32}-C_{33}	77	178	178
Mol. Mech. Energy (Kcal)	23.43	23.55	23.62
Chain #3			
C_{46}-C_{47}-C_{48}-C_{49}	−155	−176	−176
C_{47}-C_{48}-C_{49}=C_{50}	−173	177	177
C_{48}-C_{49}=C_{50}-C_{51}	0	0	0
C_{49}=C_{50}-C_{51}-C_{52}	−168	147	147
C_{50}-C_{51}-C_{52}-C_{53}	−84	−175	−175

[a]Fig. 6.

[b]Figure 7.

[c]Figure 8.

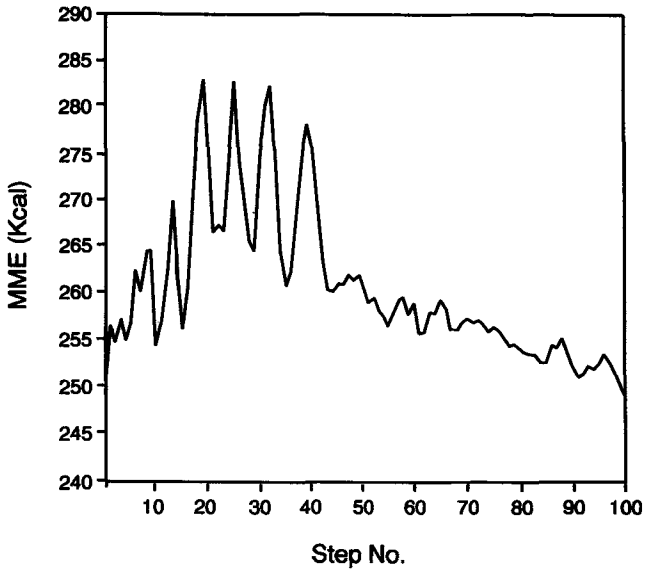

FIG 10. Molecular mechanics energy *vs.* step number for DCL to TCL conversion of SOS.

REFERENCES

1. Lutton, E.S., *J. Am. Chem. Soc. 68*:676 (1946).
2. Lutton, E.S., and F.L. Jackson, *Ibid. 72*:3254 (1950).
3. Gibon, V., F. Durant and C. Deroanne, *J. Am. Oil Chem. Soc. 63*:1047 (1986).
4. Sato, K., T. Arishima, Z.H. Wang, K. Ojima, N. Sagi and H. Mori, *Ibid. 66*:664 (1989).
5. Lutton, E.S., *Ibid. 48*:245 (1971).
6. Hagemann, J.W., and J.A. Rothfus, *Ibid. 60*:1308 (1983).
7. Allinger, N.L., *Adv. Phys. Org. Chem. 13*:1 (1976).
8. Lutton, E.S., *J. Am. Chem. Soc. 70*:248 (1948).
9. Lutton, E.S., *J. Am. Oil Chem. Soc. 49*:1 (1972).
10. Timms, R.E., *Prog. Lipid Res. 23*:1 (1984).
11. Hoerr, C.W., and F.R. Paulicka, *J. Am. Oil Chem. Soc. 45*:793 (1968).
12. Ferguson, R.H., and E.S. Lutton, *J. Am. Chem. Soc. 69*:1445 (1947).
13. Hagemann, J.W., and J.A. Rothfus, *J. Am. Oil Chem. Soc. 60*:1123 (1983).
14. Bociek, S.M., S. Ablett and I.T. Norton, *Ibid. 62*:1261 (1985).
15. Hagemann, J.W., in *Crystallization and Polymorphism of Fats and Fatty Acids*, edited by N. Garti and K. Sato, Marcel Dekker Inc., New York, 1988, pp. 16–22 and 26–73.
16. Sawzik, P., and Craven, B.M., *J. Lipid Res. 25*:851 (1984).
17. Craven, B.M., and P. Sawzik, *Ibid. 25*:857 (1984).
18. de Jong, S., Thesis, University of Utrecht, 1980, pp. 71–87.
19. Abrahamsson, S., and I. Ryderstedt-Nahringbauer, *Acta Cryst. 15*:1261 (1962).
20. Craven, B.M., *J. Phys. Chem. 63*:1296 (1959).
21. Hagemann, J.W., W.H. Tallent and K.E. Kolb, *J. Am. Oil Chem. Soc. 49*:118 (1972).
22. Larsson, K., *Ibid. 43*:559 (1966).
23. Chapman, D., *Chem. Rev. 62*:433 (1962).
24. Desmedt, A., C. Culot, C. Deroanne, F. Durant and V. Gibon, *J. Am. Oil Chem. Soc. 67*:653 (1990).

[Received June 25, 1991; accepted February 26, 1992]